

Investigation on the Inclusions in Maraging Steel Produced by Selective Laser Melting

L. Thijs & J. Van Humbeeck

Dept. of Metallurgy and Materials Engineering, Catholic University Leuven, Belgium.

K. Kempen, E. Yasa & J.P. Kruth

Dept. of Mechanical Engineering, Catholic University Leuven, Belgium.

M. Rombouts

VITO nv, Mol, Belgium

ABSTRACT: Maraging steel is an iron-nickel steel alloy which achieves its superior strength, hardness and toughness by aging the martensite phase. In earlier investigations, however, the toughness of selective laser melted (SLM) and subsequent aged maraging steel was found to be low. Several authors attribute this to the large oxides present in the finished product. In this work, the origin for these oxides is investigated by using microscopy and spectroscopy. The analysis is done on specimens produced under different processing conditions and the most important characteristics of the inclusions are discussed. It is found that during the SLM process, an oxide layer containing Al and Ti is created on top of each layer. Upon melting the next layer, the oxide layer is broken and dragged further. Therefore, accumulations of oxide material are found in the final product as large, irregularly shaped inclusions.

1 INTRODUCTION

1.1 Selective Laser Melting (SLM)

Selective Laser Melting is a powder-based additive manufacturing (AM) technique by which functional parts are produced directly from a Computer Aided Design (CAD)-model. Successive thin layers of metallic powder are melted locally upon the interaction with a laser beam. The path of the laser is determined by the cross section of the CAD-model for the layer under consideration. After the scanning of the cross section of one layer, another layer of powder material is deposited and scanned until the part is completely built. The schematic overview of the process is illustrated in Figure 1. By using high intensity laser beams, almost 100% dense, functional parts can be produced. Moreover, the CAD-based and layer-wise production allows a mass customization and high geometrical freedom. Interesting applications are the production of patient-specific implants, tooling inserts with complex conformal cooling channels and light weight supporting structures. More information about the process details, its benefits and applications can be found in Kruth et al. (2007).

1.2 Maraging steel

The maraging steels are well known for combining good material properties like high strength, high toughness, good weldability and dimensional stability

during aging heat treatment. Therefore, maraging steels are mainly used in the aircraft and aerospace industry and secondly in tooling applications. (Rohrbach & Schmidt 1990) In this research, the maraging steel grade 300, containing 18 wt% of Ni was used. The nominal composition of this maraging steel grade is given in Table 1.

Maraging steels differ from high strength conventional steels in terms of the hardening mechanism. The hardening in Maraging steel doesn't involve carbon, but is achieved by a metallurgical reaction. The relatively soft body centered cubic martensite, which is formed upon cooling, is hardened by the precipitation of intermetallic compounds at temperatures of about 480°C. (Rohrbach & Schmidt 1990)

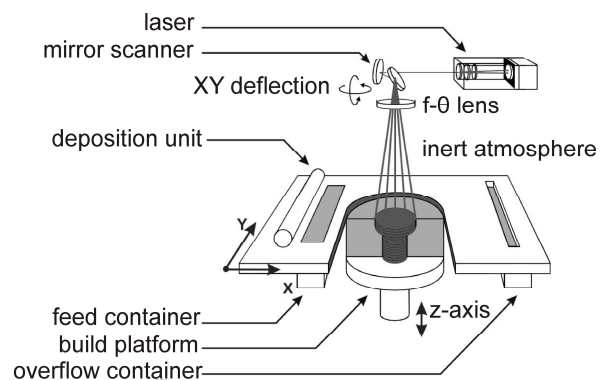


Figure 1. Schematic illustration of the Selective Laser Melting (SLM) process.

Table 1. Chemical composition of 18Ni-300 steel according to specifications DIN 1.2709.

Elements	Fe	Ni	Co	Mo	Ti	Al	Cr	C	Mn, Si	P,S
[wt%]	Bal.	17-19	8.5-9.5	4.5-5.2	0.6-0.8	0.05-0.15	<0.5	<0.03	<0.1	<0.01

1.3 SLM of Maraging steel

The microstructure of maraging steel parts produced by SLM differ significantly from the microstructure obtained after conventional production techniques, like forging, casting and milling. In the top views (see Fig. 2 left), the individual scan tracks and their scanning direction can be recognized. In the side views (see Fig. 2 right), the cross section of the melt pools can be seen. The grains consist of fine cellular dendrites ($< 1 \mu\text{m}$) and are mostly not confined to the melt pool borders.

From the pictures (see Fig. 2), it can be seen that the produced parts are almost dense. However, a lot of dark grey inclusions are present. These inclusions were previously observed in SLM parts of Maraging steel 18Ni(300) by Stanford et al. (2008), Yasa et al. (2010) and Kempen et al. (2011). In Stanford et al. (2008), these inclusions are indicated as being combined $\text{TiO}_2\text{:Al}_2\text{O}_3$ oxides.

Since the presence of large oxide inclusions is detrimental for the mechanical properties (Kiesling & Lange 1978), a closer look into these inclusions will be given in this work. The inclusions' composition, shape and location will be discussed and an insight into the formation of these will be presented.

More information about the microstructure and mechanical properties of maraging steel 18Ni(300) parts produced by SLM can be found in Stanford et al. (2008), Yasa et al. (2010) and Kempen et al. (2011).

2 EXPERIMENTAL PROCEDURES

2.1 Production

A Concept Laser M3 Linear machine was used to build the specimens (Concept Laser GmbH). This machine employs a diode-pumped Nd:YAG laser with a wavelength of 1,064 nm and a maximum laser output power of approximately 100 W measured in continuous mode. The laser beam diameter $d_{99\%}$ at the powder bed surface is about 180 μm . The powder material was supplied by LPW (M300-1) (Concept Laser GmbH).

The SLM samples were built with a set of process parameters chosen in terms of maximal density

which were derived from Yasa et al. (2010) and which are presented in Table 2. The different layers were scanned according to the island scanning pattern, which is patented by Concept Laser GmbH. (see Fig. 3). The parts were made under a N_2 atmosphere containing two different levels of residual O_2 content. During one build, the normal atmospheric conditions of the CL machine, i.e. technical pure N_2 , was applied. For this atmosphere the residual oxygen content level in the process chamber measured with a Greisinger Electronic GMH 3691 digital oxymeter placed was below 0.5 vol%. To obtain a N_2 atmosphere with higher oxygen content, ambient air was allowed to leak into the machine by stopping the build and atmosphere flushing after a few layers. As a result, an oxygen enriched N_2 atmosphere containing 1-2 vol% of O_2 was obtained. In each build, a single melted part (i.e. a part in which the layers are only scanned once) and a remelted part (i.e. a part in which the layers were scanned twice) were built.

Table 2. Overview of the applied scanning parameters which were derived from Yasa et al. (2010).

Power W	Speed mm/s	Spacing μm	Island size mm	Layer thickness μm
105	150	112*	5 x 5	30

* This is 62% of spot size $d_{99\%}$.

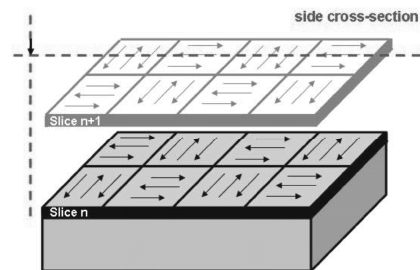


Figure 3. Illustration of the islands scanning strategy.

2.2 Materials characterization

Light optical microscope (LOM) images were made on an Axioskop 40 Pol/ 40 A Pol microscope after immersing the polished samples for 10s in a 10% Nital solution, i.e. 10% HNO_3 in ethanol. A Philips Scanning Electron Microscope XL 40 equipped with a LaB6 electron gun and Energy Dispersive X-ray Spectroscopy (EDX) system was used to make the secondary (SE) and back scattered (BSE) images and the composition measurements.

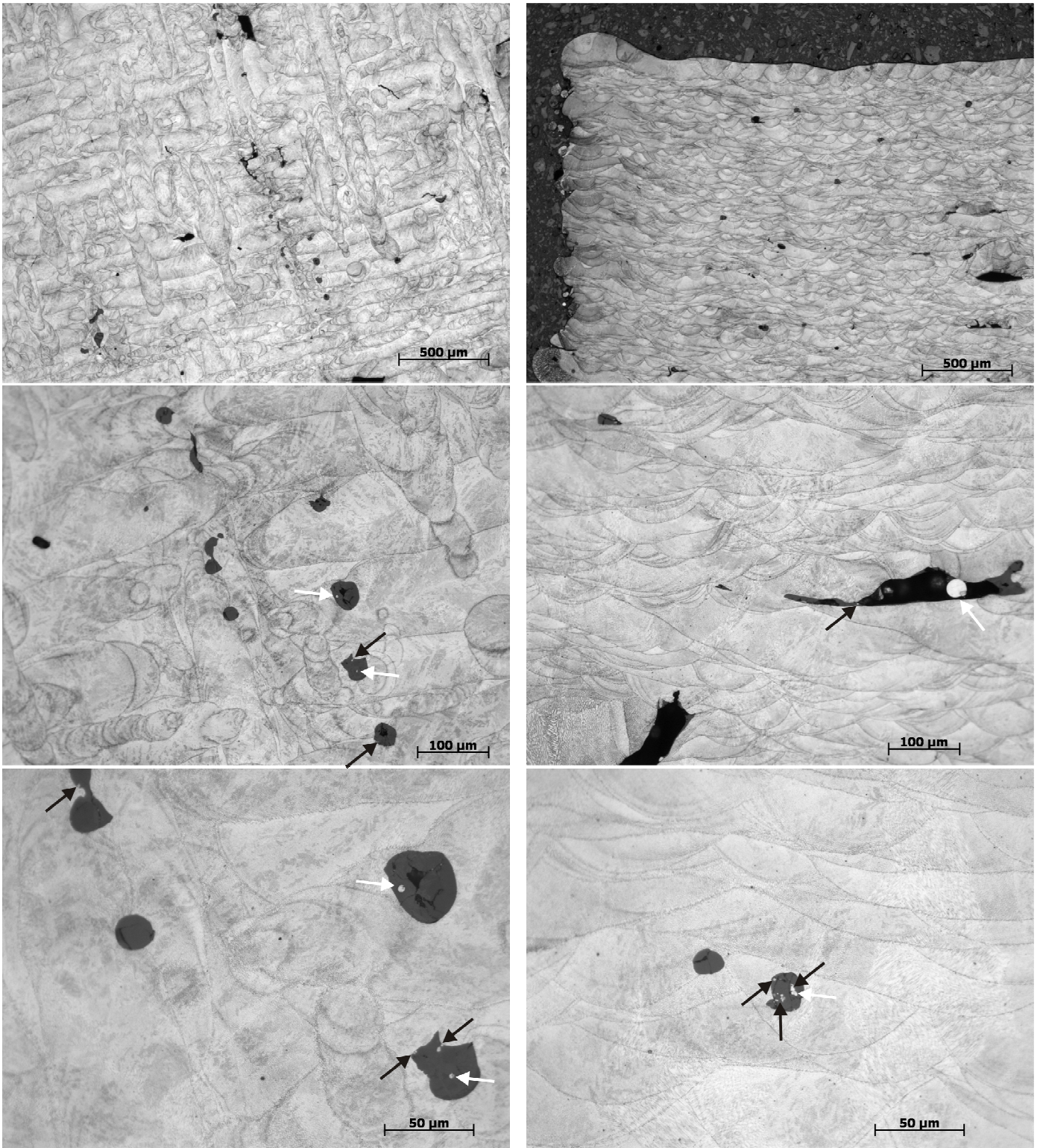


Figure 2. LOM micrographs at different magnifications of the SLM parts built with laser re-melting under technical pure N_2 atmosphere. Top (left) and side views (right) are showing the melt pool shapes and the dark grey oxides containing white parent powder particles (indicated by the white arrows) and yellow TiN inclusions (indicated by the black arrows).

For more accurate compositional measurements, Electron Probe Micro Analysis (EPMA) was performed using a JEOL JXA-8621MX apparatus. The chemical composition of the different phases was determined using a wavelength-dispersive detector (WDXA) equipped with crystals especially suited for the detection of light elements like oxygen and nitrogen.

3 RESULTS

First, the inclusions found inside the Maraging steel parts produced with SLM are described. Then, the oxides at the SLM parts' top surface are studied. Finally, the powder quality is checked.

3.1 Inclusions in SLM parts

The inclusions in the part produced under technical pure N₂ atmosphere can already be seen from the pictures in Figure 2. In Figure 4, 5 and 6, examples of inclusions produced under the oxygen enriched N₂ atmosphere are shown as well. The inclusions that are present in the SLM parts are big; the sizes range from 10 to 100 μm. Some inclusions are spherical, but the majority has an irregular and elongated shape.

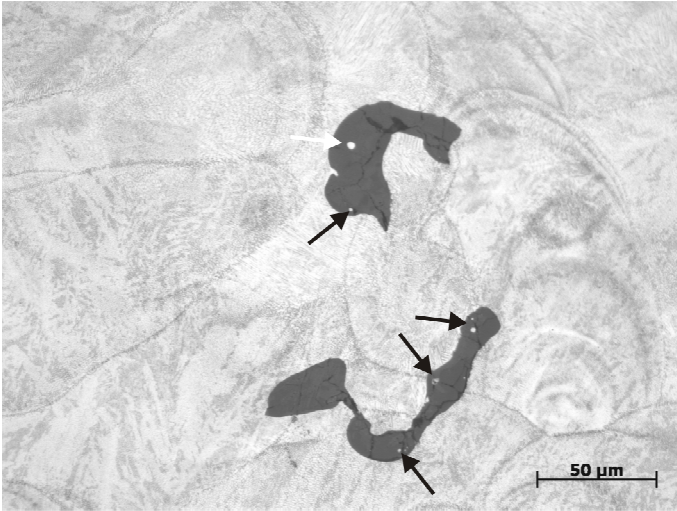


Figure 4. LOM image of the top surface of a Maraging steel part produced with SLM in N₂ atmosphere enriched in oxygen and with single melting of each layer. The white parent powder particle is indicated by the white arrow; the yellow TiN inclusions by the black arrows.

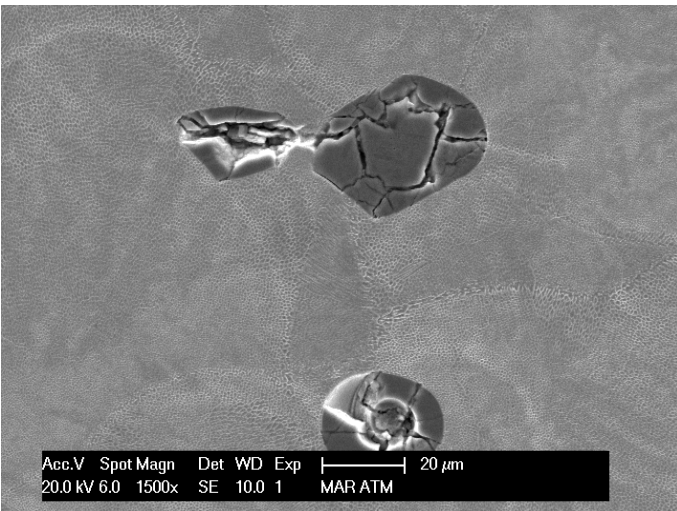


Figure 5. SE image of the top surface of a Maraging steel part produced with SLM in N₂ atmosphere enriched in oxygen and with single melting of each layer. All inclusions are heavily cracked. The lower inclusion contained a gas bubble.

In the LOM pictures using white light, these inclusions appear grey. Inside these grey inclusions, smaller white and yellow/gold colored particles can be found. The yellow particles are cubic and their size ranges from 1 to 5 μm. The inclusions also show cracks and sometimes contain air bubbles (see Fig. 5). Due to the cracking of the inclusions, some

part of the inclusion material may be removed during grinding and polishing.

At first sight, the location of the oxides seems random. But a closer look at the top views in Figure 2 point out that a higher concentration of inclusions can be found near the island borders.

The composition for an inclusion in a part produced under oxygen enriched N₂ atmosphere determined by EDX is given in Table 3. The measured inclusion is shown in Figure 6.

Table 3. EDX measurement results on different features inside an inclusion in a part produced under an oxygen enriched N₂ atmosphere with single layer melting. The measuring spots are indicated by the arrows in Figure 6. The metal particle composition is given in wt%; the inclusions' composition in at%.

Metallic particle	[wt%]	Fe	Ni	Co	Mo	Ti
Spot 1		59	20	12	6	3
Inclusions	[at%]	Ti	Al	O	N	Fe
Spot 2		29	2	63	5	1
Spot 3		25	0	34	41	/

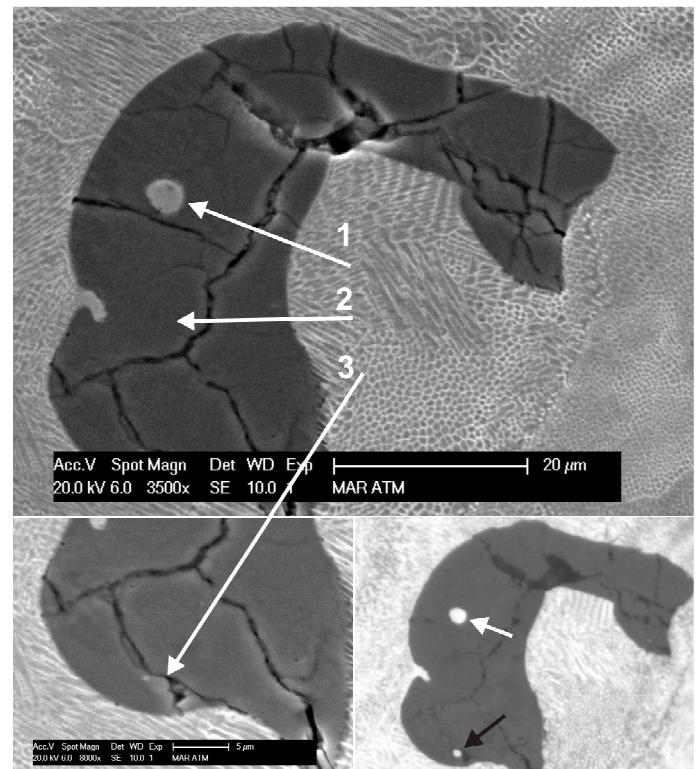


Figure 6. SE (top and bottom-left) and LOM (bottom-right) image of the top surface of a Maraging steel part produced with SLM in N₂ atmosphere enriched in oxygen and with single melting of each layer. The arrows 1, 2 and 3 are indicating the corresponding EDX measuring points. In LOM, the white parent powder particle is indicated by the white arrow; the yellow TiN inclusions by the black arrow.

It should be noted that a large electron beam size was used and therefore influence of the surrounding Fe or oxide matrix could not be avoided. Furthermore, this technique is not sensitive to light elements such as oxygen and nitrogen. Therefore, these results should only be considered indicatively. More accurate results are obtained by using EPMA, see further.

From these results, it can be deduced that the grey inclusions are Ti and Al containing oxides. The white particles embedded in the oxide inclusions are entrapped parent maraging steel powder particles. And finally, the last type of particles found in the big inclusions is TiN particles. Being TiN explains the gold color of this phase when viewed with LOM. Also the composition of other inclusions in the same SLM part as well in the parts produced under different conditions was measured. All results confirmed these findings.

EPMA measurements on various inclusions were performed to determine more accurately the exact composition of the oxide phase. This is illustrated in Table 4 for inclusions inside single melted SLM samples produced under oxygen enriched N₂ atmosphere. The presence of TiN inclusions was also confirmed by EPMA.

Table 4. EPMA results of inclusions inside a single melted Maraging 18Ni-300 steel part produced under an oxygen enriched N₂ atmosphere. The average and standard deviation of the content is given in at%.

[at%]	Ti	Al	O
O2 enriched N2	34.3 ± 0.4	3.1 ± 0.4	62.6 ± 0.3

3.2 Oxides at top surface

A closer look at the top surface in the side view of the sample produced under the N₂ atmosphere enriched in oxygen in Figure 7 reveals the presence of an oxide layer on top of the last melted layer containing the yellow TiN particles as well.

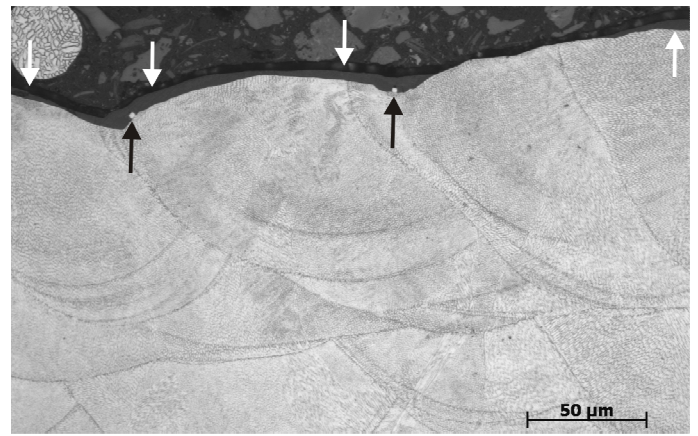


Figure 7. LOM image of the top surface in side view of a Maraging steel part produced with SLM in N₂ atmosphere enriched in oxygen and with single melting. The white arrows are indicating the oxide layer on top of the SLM part; the black arrows the yellow TiN inclusions.

Figure 8 shows the secondary electron (SE) and backscattered electron (BSE) image of the top surface of a single melted part produced under N₂ atmosphere. The individual scan tracks of the top surface can be discerned. The pictures are taken at the intersection of 4 islands. The black and white arrows in the SE graph of Figure 8 indicate the direction and order of melting the tracks of two neighbouring scanning islands. The direction of each single scan track can be deduced by the direction of the crescent-shaped solidification ripples. The order, in which the tracks were scanned, can be reasoned by the part of the crescent-shaped ripple which is covered by the neighbouring scan track.

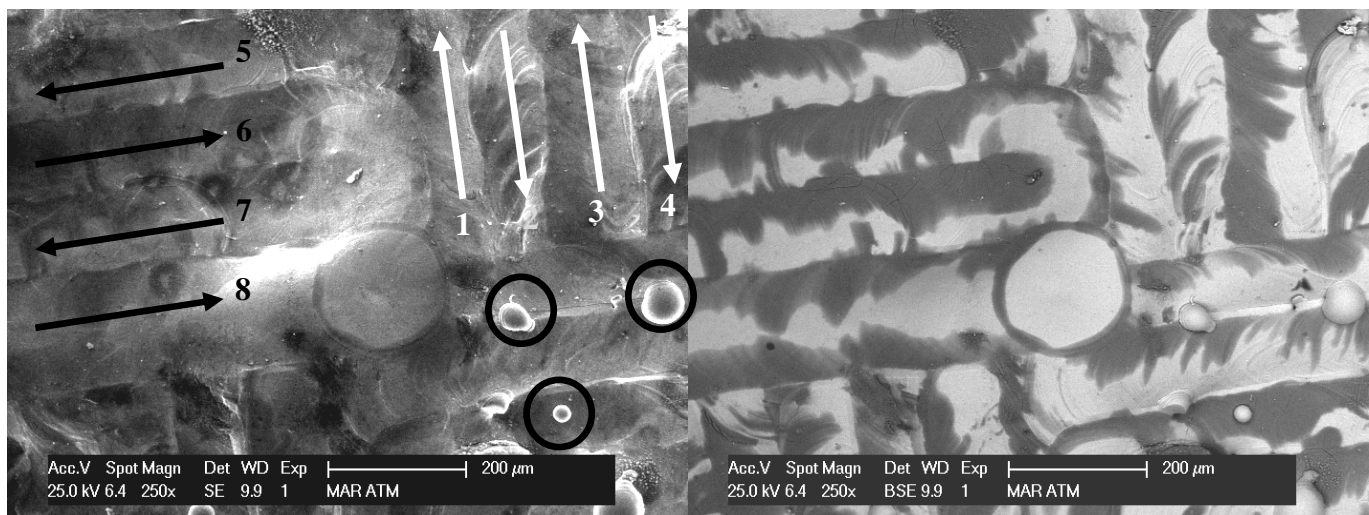


Figure 8. SE (left) and BSE (right) pictures of the top surface of a Maraging steel part produced with SLM in N₂ atmosphere and with single melting of each layer. The black and white arrows in the SE graph (left) are indicating the scanning direction for different melt tracks in two different scanning islands. The white phase in the BSE graphs (right) is the Maraging steel matrix; the dark phase which is present on top of the melt pools is an oxide layer. Maraging steel powder particles that are attached to the top surface are encircled in black.

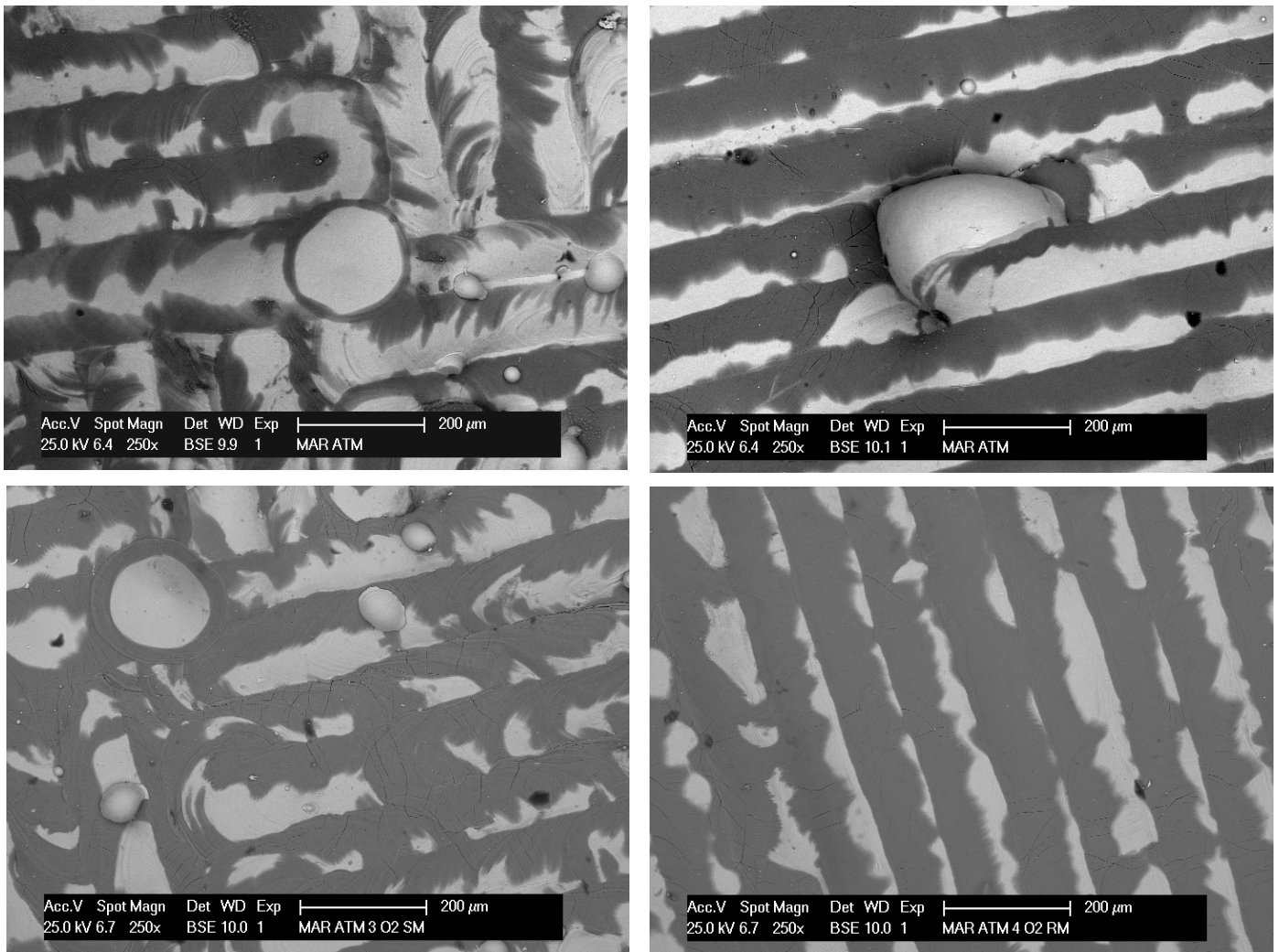


Figure 9. Backscattered Electron (BSE) graphs of the top surface of Maraging steel SLM parts in which the layers were single melted (left) or remelted (right) and produced under a technical pure N₂ (top) or an oxygen enriched N₂ (bottom) atmosphere.

The BSE graph in Figure 8 shows the presence of a second material phase on the top surface which contains lighter elements than the Maraging steel matrix. With EDX and EPMA analysis (Table 4 and 5), this phase was identified to be a Ti and Al containing oxide with the same composition as the oxides that are present in the bulk of the SLM parts.

As illustrated by the end scanning vector (track 8 in Figure 8), the oxide layer forms at both the side borders of the melt pool. For the melt pools which have a neighbouring scanned track, only part of the melt pool remains covered with the oxide layer due to the about 40% overlap between scan tracks that was applied. At the end of track 8, a circular oxide phase is seen due to the small recline when the laser beam moves to another position. Furthermore, some Maraging steel powder particles are attached to the top surface. These are indicated by the circles in Figure 8.

In Figure 9, the BSE graphs of the top surface of the parts produced under 4 different production conditions (produced under technical pure N₂ or oxygen enriched N₂ atmosphere; single or remelted each layer) are compared.

Table 5. EPMA results of inclusions at the top of single melted maraging 18Ni-300 steel parts produced under technical N₂ and oxygen enriched N₂ atmosphere. The average and standard deviation of the content is given in %.

[at%]	Ti	Al	O
N ₂	34.8 ± 0.5	3.6 ± 0.4	61.5 ± 0.5
O ₂ enriched N ₂	34.2 ± 0.7	3.1 ± 0.3	62.3 ± 0.4

In the parts produced under the oxygen enriched N₂ atmosphere, a higher surface fraction is covered by the oxide and the colour of the oxide material is more uniform. The higher oxygen level results in a higher surface coverage as well as thicker oxide layers. Thus, more oxide material is present on top of the parts produced in the oxygen enriched N₂ atmosphere compared to the parts under the technical pure N₂ atmosphere.

The shape of the oxide layer on top of the single melted scan tracks is irregular near the centre of the melt pool. The shape of the inner border of the oxide layer on top of the re-melted scan tracks is straighter.

Re-melting the just-scanned layer thus produces a more uniform width of the oxide layer.

The more fluctuating width of the oxide layer of the single scanned parts reflects the more fluctuating nature of melting powder particles compared to the more steady nature of re-melting solid material. In melting a powder layer, the heat absorption depends on the local particle size and the way of stacking.

Due to the difference in expansion coefficient, and differences in mechanical properties like E-modulus and yield strength between the oxide and metallic phase, the oxide layer on top of the melt pool is cracked. This can be seen more clearly for the thicker oxide layers produced under the oxygen enriched atmosphere (see Fig 9 bottom).

3.3 Powder material

To find a cause/origin for the presence of the oxides and nitrides, the used powder material quality was checked.

In Figure 10, a SEM micrograph of the recycled, gas atomized powder is given. The powder particles are nicely spherical and in between the powder particles no oxide material was found. The powder material is not introducing exogenous contamination into the powder bed.

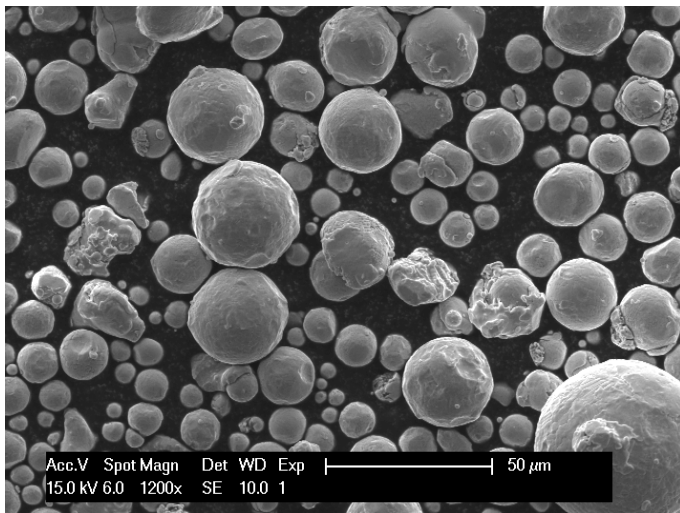


Figure 10. SEM picture of the recycled Maraging steel powder that was used for building the SLM parts.

4 DISCUSSION

In the layer-based manufacturing techniques, one of the most important parameters is the condition of the top layer of the part being created. During the process, each top surface of the just added layer is the substrate for the next layer to be built. From this research it can be seen that the formation of an oxide layer on top of the melted tracks results in the formation of big oxide inclusion in the bulk of the maraging steel 18Ni(300) SLM parts.

The oxide layer is formed by the oxidation of the alloying elements with the highest affinity to oxygen. In maraging steel 18Ni(300), Ti and Al have the highest affinity to oxygen (Hong et al. 2000, Hong and DebRoy 2001), so it shouldn't be a surprise to find these elements in the oxide phase created here. These elements are oxidized by reaction with the solute oxygen inside the melt pool. Due to the lower density of the oxides compared to the liquid melt, the oxide material will float. Although the oxide phase is generally more stable than the nitride in the steel melt, part of the Ti from the Maraging steel reacts with nitrogen to form small, cubic, yellow TiN particles. It is seen from Hong and DebRoy (2001) that at low temperatures (i.e. 1700K), growth of TiN inclusions is faster than of the oxides. The growth of TiN is most likely encouraged by the high N₂ supply from the atmosphere.

The atomic percent ratio of Ti and Al inside the oxides found in the maraging steel 18Ni(300) SLM parts is 90 to 10. This is comparable to the ratio of Ti and Al in the Maraging steel alloy (see Table 2).

From various studies in literature, it is known that the most stable Al oxide in steel is the Al₂O₃ phase (Hong2000, Hong2001, Babu1995). Ti can bond with oxygen in different ratios depending on the temperature and partial pressure of oxygen. Based on the EPMA results of the oxide layer, the best correspondence was found with the Ti₃O₅ phase. This is shown in Figure 11 where the solid lines are the theoretical ratio's of Ti and O in various oxides while the data points represent the experimentally measured composition.

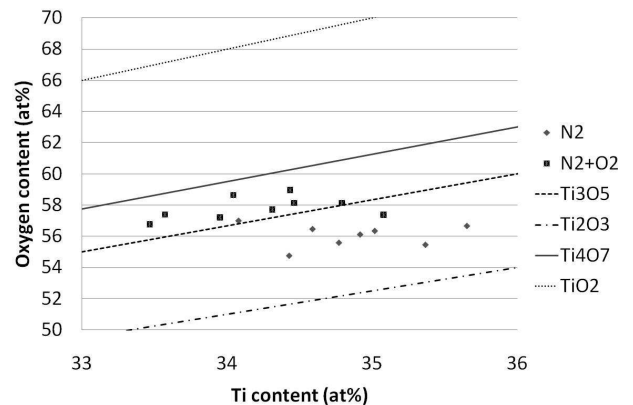


Figure 11. Data points representing the titanium and remaining oxygen content in the inclusions of single melted SLM parts built in N₂ and oxygen enriched N₂ atmosphere, assuming that all the aluminum in the inclusions is present as Al₂O₃. The solid lines represent the theoretical content for various types of oxides.

The highest stability of Ti₃O₅ in molten steels is also reported in other studies (Hong et al. 2000). It should be noted that for the oxygen enriched N₂ atmosphere the results tend to deviate from Ti₃O₅ towards oxides with higher oxygen content, while the

opposite deviation is observed for N₂ atmosphere. These results are in line with the expected trend as a function of partial pressure of oxygen. These findings indicate that during SLM of Maraging steel 18Ni(300), a combined oxide phase containing mainly Ti₃O₅ and Al₂O₃ is formed. Furthermore, a trend towards more Ti₂O₃ when producing under a lower oxygen partial pressure can be seen. This shift is also expected based on the known Ti-O binary phase diagrams.

The oxide material on top of the melt pool is only present at the sides of the melt pool surface. This is also observed during Ar-O₂ GTA welding of stainless steel. (Lu et al. 2004) The melt pool is known to have a large temperature gradient across the surface. The driving force for oxide formation is higher at lower temperature, so higher at the periphery than in the centre of the melt pool. Also, as shown in Hong and DebRoy (2001), an equilibrium temperature exists for a given metal oxide-steel system. Above this temperature no metal oxides will grow and/or the existing ones will dissolve. Due to the extremely fast cooling rates during SLM (i.e. more than 10³ K/s), it is assumed that no further significant oxidation takes place upon solidification and further cooling. Therefore, the oxides are formed at the periphery of the melt pools.

In addition, at relatively low oxygen contents in the melt pool an outward Marangoni flow exists at the surface of the melt pool (see Figure 12(a)). This flow may destroy the oxide layer and drag it (further) towards the sides of the melt pool. However, due to the oxygen take up during SLM, the oxygen content in the melt pool may increase and causes the flow in to become inward (Figure 12(b)).

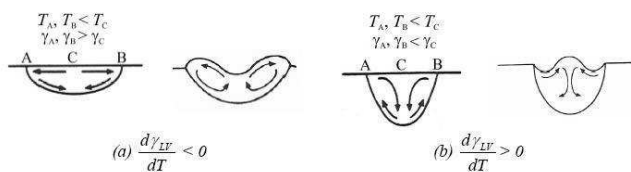


Figure 12. Schematic representation of the Marangoni flows due to a temperature gradient at the surface of a melt pool for a material with a negative (a) and a surface with a positive surface tension gradient (b). (Mills et al. 1998)

During selective laser melting of the maraging steel, part of the previously melted layer is re-melted to assure a good adhesion between the successive layers. During this re-melting, the cracked oxide layer is broken up and taken away with the moving melt pool. Like mentioned before, the oxide material will tend to float on top of the new melt pool due to the difference in density. However, part of the material may become entrapped and accumulates into large inclusions wrapped by the melt pools. Hereby, it is also possible to trap powder particles or gas

bubbles inside the oxide inclusion as seen in Figures 4, 5 and 6.

5 CONCLUSIONS

During SLM of Maraging steel 18Ni(300) under technical pure N₂ and oxygen enriched N₂ atmosphere an oxide layer containing TiN particles is formed on top of the SLM part. This oxide layer is composed of Al₂O₃ and mainly Ti₃O₅. The ratio between the Ti and the Al oxides is about 85:15. The amount of oxide layer is seen to increase with higher oxygen content in the atmosphere and upon layer re-melting. When proceeding the SLM process by melting the next layer, the oxide layer is broken up. Part of this oxide material will float on top of the newly formed melt pools; part of it will be trapped inside the SLM part. Especially when the scan track changes direction, oxide material is prone to be left as big oxide inclusions. The inclusions present in maraging steel 18Ni(300) SLM parts are big (10 – 100 μm) and irregular of shape. The inclusions contain the same oxide material as the layers that were created on top of the melt pools. Furthermore, they also contain smaller yellow TiN particles, parent maraging steel (powder) particles and gas bubbles.

In this article, an explanation for the formation of the big oxide inclusions containing small TiN particles found in Maraging steel 18Ni(300) SLM part. The atmosphere during the SLM of maraging steel 18Ni(300) turns out to be play an important role. Further investigations should be performed by using atmospheres low in oxygen and nitrogen like argon or argon-helium mixtures or producing under vacuum conditions.

6 REFERENCES

- Babu, S.S., David, S.A., Vitek, J.M., Mundra, K. and DebRoy, T. 1995. Development of Macro- and Microstructures of C-Mn Low Alloy Steel Welds – Inclusion Formation. *Materials Science and Technology*, 11(2), 186-199.
- Concept Laser GmbH/ M3 Linear, *Web-Based Data, Concept Laser GmbH Co.*, Germany, <http://www.concept-laser.de/>, as 29.04.2011.
- Hong, T., DebRoy, T., Babu, S.S., David, S.A. 2000. Modeling of inclusion growth and dissolution in the weld pool. *Metallurgical and Materials Transactions B*, 31B(1), 161-169.
- Keene, B.J. 1998. *Review of data for the surface tension of iron and its binary alloys*. International Materials Reviews, 33(1), 1-37.
- Hong, T. and DebRoy, T. 2001. Effects of time, temperature, and steel composition on growth and dissolution of inclusions in liquid steels. *Ironmaking and Steelmaking*, 28(6), 450-454.
- Kempen, K., Yasa, E., Thijs, L., Kruth, J., Van Humbeeck, J. (2011). Microstructure and mechanical properties of Selec-

tive Laser Melted 18Ni-300 steel. In *Proceedings of the Lasers in Manufacturing (LIM) 2011*, Munich, 23-26 May 2011.

Kiesling, R., Lange, N. 1978 Non-metallic inclusions in steel. Bournemouth: The Metals Society.

Kruth, J., Levy, G., Klöcke, F., Childs, T. 2007. Consolidation phenomena in laser and powder-bed based layered manufacturing. *CIRP Annals-Manufacturing Technology*. 56 (2), 730-759.

Mills, K.C., Keene, B.J., Brooks, R.F., Shirali, A. 1998. Maragonif effects in welding. *Philosophical Transactions: Mathematical, Physical and Engineering Sciences*. 356(1739), 911-925.

Rohrbach, K. & Schmidt, M. 1990. Maraging Steels, *Properties and Selection: Irons, Steels, and High-Performance Alloys*, ASM Handbook, ASM International, Vol 1: 793-800.

Stanford, M. Kibble, K., Lindop, M., Mynors, D. and Durnall, C.. 2008. An investigation into fully melting a maraging steel using direct metal laser sintering (DMLS). *Steel research int. Special Editions Metal forming Conference 2008*. 79(2):847-852.

Yasa, E., Kempen, K., Kruth, J., Thijs, L. and Van Humbeeck, J. 2010. Microstructure and mechanical properties of maraging steel 300 after Selective Laser Melting. In *Solid Freeform Fabrication; Proc. Intern. Conf., Austin(Texas), 12-14 August 2010*.

7 ACKNOWLEDGEMENTS

The authors acknowledge the “Catholic University Leuven (K.U.Leuven)” for support through the Project GOA/2002-06 and the “Agency for Innovation by Science and Technology in Flanders (IWT)” for support through the DiRaMaP Project. The latter institute is also thanked by Lore Thijs for providing a doctoral bursary.